Peer-reviewed version available at *Materials* **2020**, *13*, 3231; doi:10.3390/ma13143231

Review

A mini review on lanthanum ferrites-based exsolved perovskites as fuel-flexible anode for Solid Oxide Fuel Cells

Massimiliano Lo Faro*, Sabrina C. Zignani, and Antonino S. Aricò

CNR-ITAE, Istituto di Tecnologie Avanzate per l'Energia "Nicola Giordano", Via Salita S. Lucia sopra Contesse 5 - 98126 Messina, Italy; lofaro@itae.cnr.it (M.L.F.); zignani@itae.cnr.it (S.C.Z.); arico@itae.cnr.it (A.S.A.)

* Correspondence: lofaro@itae.cnr.it; Tel.: +39 090624243

Abstract: Exsolved perovskites can be obtained from lanthanum ferrites, such as $La_{0.6}Sr_{0.4}Fe_{0.8}Co_{0.2}O_3$, as result of Ni doping and thermal treatments. Ni can be simply added to the perovskite by an incipient wetness method. Thermal treatments include calcination in air (e.g., 500 °C) and subsequent reduction in diluted H_2 at 800 °C to favor the exsolution process. The chemistry of the nanoparticles exsoluted on the substrate surface can be further modulated by a post treatment in air. These processes allow to produce a two-phase material consisting of a Ruddlesden-Popper type structure and a solid oxide solution e.g. α-$Fe_{100-y-z}Co_yNi_zO_x$ oxide. The formed electro-catalyst shows sufficient electronic conductivity under reducing environment at the SOFC anode. Outstanding catalytic properties are observed for the direct oxidation of dry fuels in SOFCs, including H_2, methane, syngas, methanol, glycerol and propane. This anode electrocatalyst can be combined with full density electrolyte based on Gadolinia-doped Ceria or with $La_{0.8}Sr_{0.2}Ga_{0.8}Mg_{0.2}O_3$ (LSGM) or $BaCe_{0.9}Y_{0.1}O_{3-\delta}$ (BYCO) to form a complete perovskite structure-based cell. Moreover, the exsolved perovskite can be used as a coating layer or catalytic pre-layer of a conventional Ni-YSZ anode. Beside the excellent catalytic activity, this material also shows proper durability and tolerance to sulphur poisoning. In this mini review, preparation methods, physico-chemical characteristics, surface properties of exsoluted and core-shell nanoparticles encapsulated on the metal-depleted perovskite substrate surface, electrochemical properties for the direct oxidation of dry fuels and related electrooxidation mechanisms are examined and discussed.

Keywords: Perovskite; Electrooxidation; Fuel flexibility; Renewables; Anode

1. Introduction

Achieving fuel flexibility in Fuel Cells has been a focus of high temperature fuel cells since their discovery [1,2]. As Solid Oxide Fuel Cells (SOFCs) operate at temperatures close or higher than 800 °C, their thermodynamics allow the direct use of dry organic fuels or organic fuels in combination with water [3]. Practical operation however requires pre-treatment of organic fuels to convert hydrocarbon and remove sulphur traces [4]. In parallel to the discovery of new materials and novel cell designs have allowed to reduce the operating temperature to 600 - 800 °C [5,6]. Several studies have concerned with the development of novel materials [7,8], and in particular novel anodes for advanced SOFCs operating in fuel-flexible mode [9-13].

Fuel flexibility is treated in this review article in relation to a specific category of electrocatalysts. Although novel SOFCs designs and several new materials have been investigated , Ni in combination with Yttria-stabilized Zirconia (YSZ) still represent today the selected approach for the anode. This because the Ni-YSZ cermet provides as a proper trade-off in terms of electrochemical, thermal and mechanical properties [14-21]. In particular, mechanical and thermal properties of Ni-YSZ are rather flexible and adequate to the production-chain of anode-supported SOFC cells [22,23]. However, the degradation of Ni-YSZ anodes during SOFC operation is frequently reported. This occurs due to the

coarsening of Ni particles [15] and to the carbon deposition [19]. Moreover, another drawback is related to the risk of Ni poisoning due to sulphur contaminants and pore blocking associated to the deposition of carbon tar [24-26]. Accordingly, large SOFC systems include a fuel pre-reformer and a desulphurizer [14,27-29]. An alternative strategy for SOFC systems simplification, quite recently adopted, consists on the use of a functional layer coated on the external side of Ni-YSZ anodes [30]. Due to the favourable electronic properties, Ni alloys in combination with doped ceria electrolyte have been widely investigated to replace bare Ni [31-33]. The specific advantage relies on a breaking effect of the crystallographic arrangement Ni atoms which is responsible for the cracking mechanism of hydrocarbons [34,35]. This effect has been achieved by the inclusion of a different transition metal, not adsorbing carbon, into the reticular scaffold of Ni. The metals selected for this inclusion were somehow inert towards the cracking reaction (e.g., Cu) [31] or capable to modify the surface electronic density and the lattice distances of the regular Ni-Ni crystallographic network (e.g., Co) [32], or a combination of all these effects (e.g. Fe)[33]. A further optimization has been then achieved by adopting different synthesis methods with the aim to improve the homogeneity of the solid solution and consequently to reduce the probability of Ni-Ni bonds occurrence on the surface[35].

Moreover, specific catalyst functionalization has been made by increasing its oxygen storage capability[36], e.g. by adding oxygen storage additives such as ceria. This is particularly desired to promote the oxidation of a fuel and to extend the "triple phase boundary" [37]. These are the sites where the electrochemical reactions take place. Thus, the alloy is generally mixed with doped ceria which is a well known material oxygen storage material as consequence of its peculiar redox properties [10]. Although this approach has been revealed promising for the direct use of dry organic molecules in SOFCs[38,39], there are, to date, limited evidences about the resistance of these Ni alloy-ceria composite catalysts towards sulphur poisoning.

An approach combining both sulphur resistance and organic fuel oxidation capabilities consists of the use of exsolved perovskites at the anode [40]. The idea of using perovskites at the anode is more recent. It raised from a large evidence about their activity towards the cleavage of C-H, C-C, and C=C bonds[41,42] with a relatively good stability in the presence of sulphur based products [43,44]. These systems are also characterized by mixed electronic and ionic conductivity [45], even if the electronic conductivity is not comparable to that of a metal also at the high operating temperatures of a SOFC. On the other hand, the perovskites may present the drawbacks of a limited structural stability under the reducing environment of a SOFC anode [46,47]. To address this issue, modification of perovskites ex-ante with the aim to functionalize their surface and tailor the activity for the anodic reactions, while stabilizing the structure and improving the electronic conductivity has been carried out [40,48]. A further step forward in tailoring these perovskite materials for the use as anode in SOFCs is relying the addition of ceria to increase the oxygen storage capacity and the electronic/ionic percolation.

The authors of this mini-review have intensively worked on modified and exsolved perovskite for application as anode in SOFCs for several years demonstrating an effective oxidation of various organic fuels directly fed to the cell [49-56]. Proper modification of commercial type ferrite-based perovskites commonly used as a SOFC cathode with small amounts of Ni has been demonstrated. The process has been enhanced by tailoring the thermal treatments to consolidate the modified perovskite structure. In this mini-review, we have summarized the properties of this novel anode materials, their performance in SOFCs and the specific reaction mechanisms investigated through a combination of electrochemical experiments and the chromatographic analyses of effluents.

2. Surface exsolution and physico-chemical studies

The exsolution of fine particles from the perovskite surface is an approach recently used for funzionalisation of peroskite materials for anodic applications [57-59]. Two main approaches have been developed: i) synthesis of a non-stoichiometric perovskite [60] and ii) surface impregnation of a raw perovskite with a foreign transition element [61,62]. Final modification is thermal driven by a process under reducing condition at high temperature in order to achieve a proper thermodynamic stability for the fine exsolved nanoparticles embedded in the perovskite substrate. The latter remains deficient of cations in A and B sites. Both approaches have been addressed to promote a similar

distribution of fine exsolved particles on the surface. It was reported that the first method should be preferred in case of high risks for their coarsening [63].

Many exsolved perovskites have been synthesized using these approaches, for various applications and with the aim to functionalize the surface of these materials. One of the most used application has regarded their use as a novel anode for SOFCs. The subject of this mini-review is specifically addressing the modification of ferrite-based perovskites commonly used as cathode in commercial type SOFCs operating in the temperature range between 700° and 800 °C. This type of perovskite has generally the formula $La_{0.6}Sr_{0.4}Fe_{0.8}Co_{0.2}O_3$ (LSFC). The raw LSFC that we have largely used in our previous works had a surface of 5.20 $m^2 g^{-1}$ and was commercialized by Praxair. By using a wet impregnation method, an aqueous solution usually containing 3% of Ni as Ni nitrate (Sigma Aldrich) has been deposited drop-by-drop on the perovskite and this was maintained under stirring condition at 80 °C. After drying at 150 °C for 8 h, the powder has been treated at 500 °C in static air for 2 h and then reduced with 5% of H_2 in N_2 at 800 °C for 2 h and then re-calcined at 500 °C in static air for 2 h to stabilize the nanoparticles on the surface. The subsequent step consisted in the grinding for 12 h this powder together with gadolinia-doped ceria ($Gd_{0.1}Ce_{0.9}O_2$-GDC, Praxair) with a surface area of 38.92 $m^2 g^{-1}$. The doping of perovskite with Ni and its subsequent thermal treatments caused a modification of the initial perovskite phase originated from the depletion of Co and Fe with the consequent formation of a new phase named as n=1 Ruddlesden-Popper ($A_{n+1}B_nO_{3n+1}$) structure [64]. Figure 1 shows the XRD spectra of the raw and modified perovskites. Fe and Co are located into the blue octahedrals, green spheres are related to the sites of La and Sr, whereas the red spheres are the sites for oxygen ions. As consequence of perovskite distortion, the ratio La/Sr (0.6/0.4) remained the same during the perovskite modification, whereas the Fe/Co ratio was altered as consequence of the Co and Fe depletion from the bulk and their migration to the perovskite surface (the Fe/ Co ratio was originally 4 in the raw perovskite). The overall amount of Ruddlesden-Popper n=1 phase was approximately 60 wt.% as determined through a least-square fitting profile quantitative analysis procedure. As evidenced by previous TEM and EDS analyses [55], the secondary phase is related to fine core-shell particles encapsulated on the surface. These are composed of a tri-metallic alloy (e.g. Ni-Fe-Co) in the core and a shell of mixed oxides (e.g. α-$Fe_{100-y-z}Co_yNi_zO_x$). Smith et al.[65,66] have reported that this mixed oxide has shown reversible electrochemical behaviour starting from low temperatures. Accordingly, it has been also suggested as a substitution of noble metals for the water electrolysis in zero-gap cells [65,66].

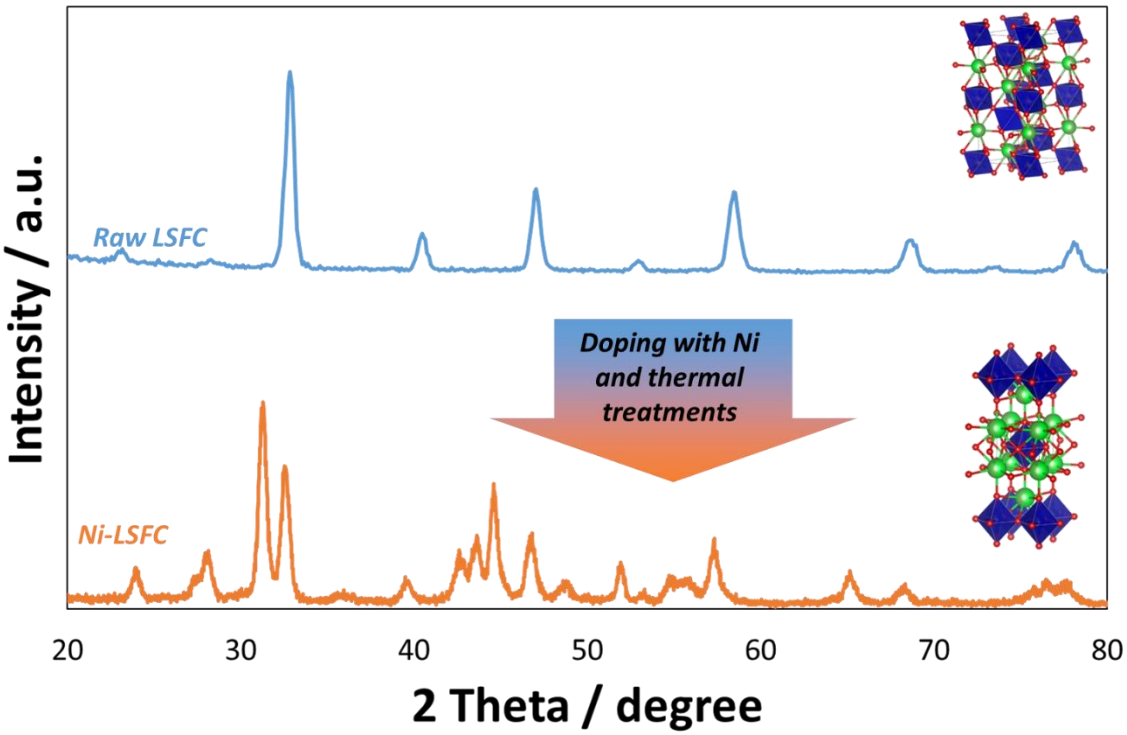

Figure 1. Structural analysis of raw (top) and modified (bottom) perovskites. The figure also reports the related unit cells. As shown, the addition of Ni and subsequent thermal treatments (calcination at 500 °C and reduction at 800 °C) caused the intercalation of one rocksalt-type phase into the perovskite (n=1 Ruddlesden-Popper phase).

The redox properties of these modified perovskites and their exsoluted fine particles have been the object of specific studies [50]. Figure 2 shows the TPR profile of Ni-LSFC/CGO, the TEM image of a fine particle encapsulated in the surface of the catalyst and its EDS analysis. As discussed, Co and Fe were alloyed with Ni and migrated to the surface of perovskite as proved by the EDS analysis, whereas an oxide shell was confirmed by the combination of EDX and TEM analysis. This peculiar structure imparts to the material outstanding catalytic properties [….]. The TPR profile showed three signals in the range of temperature 300-650 °C related to the chemisorption of H_2 on each of Co (α_1 [67]), Fe (α_2 [68]) and Ni (α_3 [69]). This indicates that the oxide surface of these nanoparticles turns into a trimetallic system under operation in reducing conditions at high temperature. The TPR profile showed also a broad peak around 650 °C which is due to the reduction of Ce ($Ce^{4+} \rightarrow Ce^{3+}$, α_4 [70,71]). Based on the XPS studies [55], the most probable oxidation states of metals for the fine embedded particles was 3^+ both the cobalt and the iron and 2^+ for the nickel. By integrating the three TPR peaks observed in the temperature range between 300-650 °C, the following composition α-$Fe_{23}Co_{15}Ni_{12}Ox$ is derived suggesting an excess of iron in line with the evidence of the EDX profile.

Preprints (www.preprints.org) | NOT PEER-REVIEWED | Posted: 12 June 2020 doi:10.20944/preprints202006.0152.v1

Peer-reviewed version available at Materials 2020, 13, 3231; doi:10.3390/ma13143231

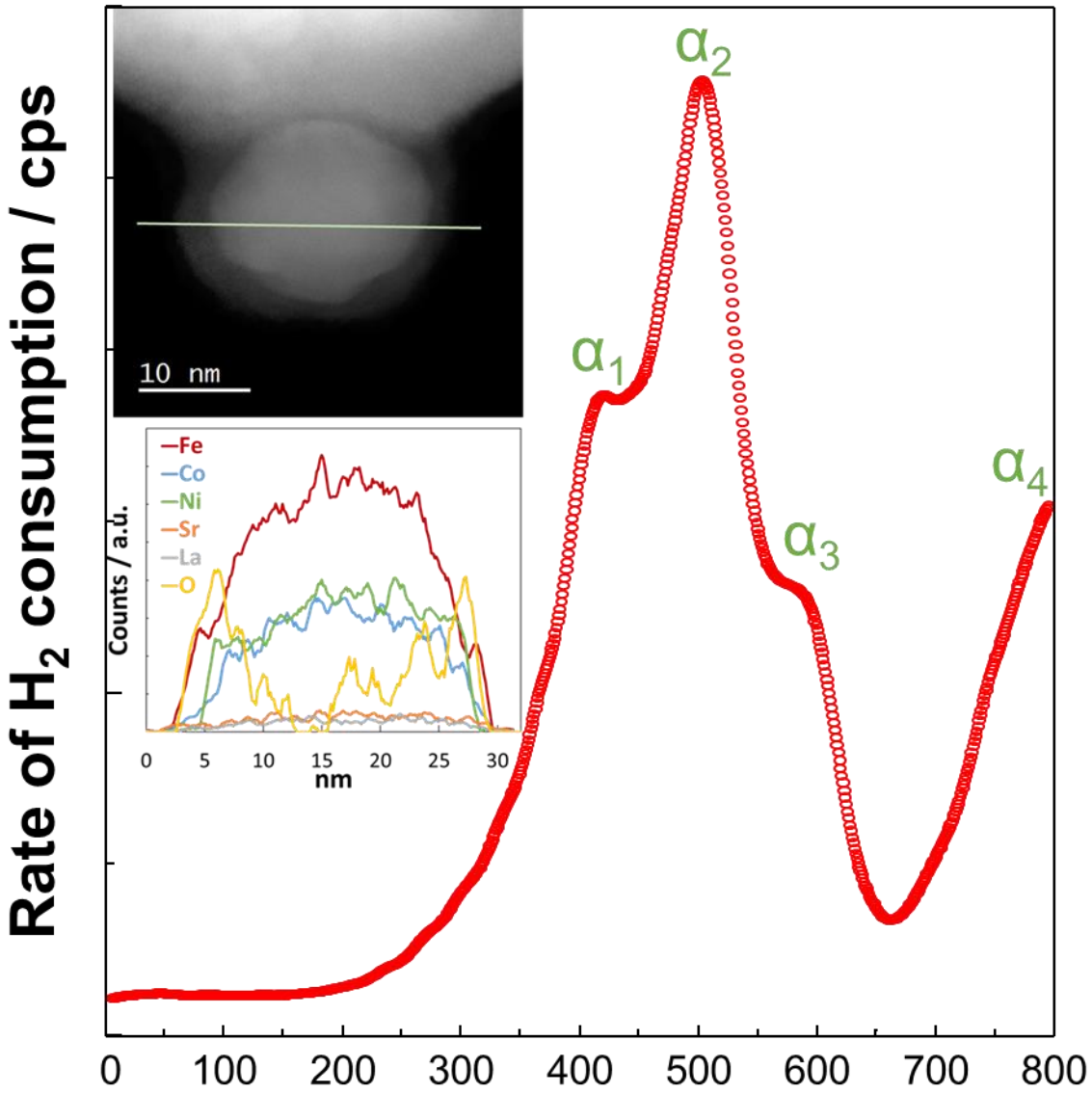

Figure 2. TPR profile of Ni-LSFC/CGO, TEM image and the EDS measure carried out along the profile of an embedded nanoparticle on the surface of a modified perovskite.

Generally the surface area of these exsolved perovskite materials is 5.51 $m^2 g^{-1}$ as evaluated by BET analysis with mesoporous morphology [51]. Thus, the formation of fine embedded particles does not promote a significant increase of the overall surface roughness for the modified perovskite catalyst being the initial surface area quite similar (e.g. 5.2 $m^2 g^{-1}$).

3. Catalytic studies

As this catalyst was suggested for the electrochemical conversion of organic fuels in SOFCs, preliminary catalytic tests have been carried out to collect information concerning its reliability towards the most common reactions occurring in the anode compartment of a SOFC during its operation. It has been largely reported that the most frequent reactions occurring at the anode compartment fed with organic fuels can be simulated ex-situ by the autothermal reaction (ATR)[72,73]. In particular, water beside CO_2 is formed during the oxidation of organic fuels and oxygen is provided at the electrolyte-anode interface. Nevertheless, some specific differences exist

between the ATR reaction and the electrochemical reaction. This essentially concerns the fact that molecular oxygen is supplied during the ATR whereas ionic oxygen is involved in the redox process. Thus, the net reactions of an electrochemical process and ATR reaction are similar but with the difference that the electrochemical reaction involves ionic oxygen and release of electrons into the external circuit. It has been discussed in the literature as a SOFC may be fed with oxygen or water in combination with organics in order to minimize the risks associated to the carbon fibers deposition (i.e. Partial Oxidation Reaction (POX)[74,75], Steam Reforming (SR)[74,76], and a combination of dry reforming and ATR named as tri-reforming [77,78],respectively). Although a right balance of the stoichiometry may effectively minimize this risk, other aspects associated to the dilution of fuel, lower efficiency and re-oxidation of the anode have suggested to avoid the in-situ supply of molecular oxygen [4,76,79-82].

Generally, the risk of damaging a SOFC increases with the increasing of the carbon atoms in the fuel molecule. This can be mitigated by varying the steam to carbon and the oxygen to carbon ratios. Therefore, the catalytic behavior of the exsolved perovskite materials has been preliminarily investigated under POX, SR and ATR of methane[52], methanol[51], propane[52] and glycerol[50]. According to such previous studies, their reactivity towards oxidation follows this trend: methanol > ethanol > propane > glycerol > methane (table 1). In particular, it has been shown [52] that methane did not reach much at 800 °C whereas other organics showed a significant production of syngas, with a H_2/CO ratio that varied according to the H/C ratio in the fuel. The same work also reported that the presence of unreacted fragments (i.e. CH_4) was depending on the molecular weight of the fuel. In addition, contrarily to what reported in the literature for the propensity of LSFC to catalyze the oxidative coupling of methane[47], no C2 compound has been detected in the outlet stream.

Specific works in the literature have addressed the stability of the perovskite in the presence of sulphur contaminants. Exsolved perovskite was investigated for the ATR of propane in presence of H_2S up to 80 ppm. These studies [53] showed as the increase of sulphur in the feed, caused a depletion of H_2 in the produced syngas and a decrease of propane conversion, since H_2S has blocked the active sites of the electrocatalyst. Nevertheless, the overall negative effects caused by the H_2S appeared to be reversible since the spent catalysts did not show any significant changes in their structure as revealed by XRD as well as limited amount of carbon and suphur contents was detected through the elemental analysis (CHNS-O). The catalysts could be, in principle regenerated by proper activation.

Table 1. Survey of the average product formation achieved in different reaction processes at 800 °C

		H_2 %	CO %	CO_2 %	CH_4 %	C_2H_4 %	C_3H_8 %	Others %	Selectivity to Syngas %
SR-800°C	Glycerol (S/C=0.2)[50]	29.45	28.39	32.90	7.50	1.76	-	-	-
SR-800°C	Glycerol (S/C=2)[50]	80.79	5.60	2.36	5.82	5.43	-	-	-
ATR-800°C	Methane (S/C=2.5; O/C =0.5) [52]	5.95	2.19	1.62	85.68	-	-	-	-
ATR-800°C	Methanol (S/C=2.5; O/C =0.5) [51,52]	67.44	13.73	17.71	0.56	-	-	-	87.42
ATR-800°C	Propane (S/C=2.5; O/C =0.5) [52,53]	66.59	17.40	4.94	6.98	2.35	0.97	0.77	-
ATR-800°C	Glycerol (S/C=2.5; O/C =0.5) [52]	31.10	29.62	29.01	9.56	-	-	-	-
SR-800°C	Methanol (S/C=2.5)[51]	-	-	-	-	-	-	-	81.70
POX-800°C	Methanol (O/C=0.5)[51]	-	-	-	-	-	-	-	92.02
SR-800°C	Propane (S/C=2.5)[53]	64.59	15.04	9.34	6.75	1.99	1.48	0.81	-
POX-800°C	Propane (O/C =0.5)[53]	43.73	29.20	0.68	13.03	10.06	1.68	1.62	-
ATR-800°C	Propane (S/C=2.5; O/C =0.5) + 20ppm H_2S[53]	22.38	8.73	18.76	15.48	28.57	6.18	-	-

ATR-800°C	Propane (S/C=2.5; O/C =0.5) + 40ppm H_2S[53]	23.97	10.29	18.07	16.28	25.02	6.37	-	-
ATR-800°C	Propane (S/C=2.5; O/C =0.5) + 60ppm H_2S[53]	14.41	10.62	19.75	15.91	26.38	10.14	2.79	-
ATR-800°C	Propane (S/C=2.5; O/C =0.5) + 80ppm H_2S[53]	13.25	8.76	19.60	16.55	29.06	12.74	0.04	-

4. Electrochemical studies

According to the ex-situ catalytic studies the modified perovskites appear a promising catalyst for application in a fuel-flexible SOFC. This material has been investigated extensively in two main cell configurations consisting a single fuel electrode supported on three different types of supporting electrolytes (e.g. CGO [49], LSGM [54]and BYCO) and as a functional layer (pre-layer) for the anode of a commercial type cell (ASC-400B, ELCOGEN[55,56]). In the latter case, the SOFC consists of a dual-anode configuration where the modified perovskite acts as a catalytic pre-layer for the conversion of the organic molecules before these can reach the supporting Ni-YSZ anode.

The electrochemical experiments for the modified perovskite-based SOFC, carried out in H_2, are reported in the figures 3a and 3b. The polarization curves (figure 3a) reveal as the highest performance has been achieved by using the exsolved perovskite as a protective or pre-layer layer in an anode supported cell configuration. The latter was based on the ASC-400B-Elcogen commercial cell simply modified by coating the exsolved perovskite on the outer anode surface. The highest performance achieved with the modified Elcogen cell is essentially due to a combination of lower ohmic constrain and higher open circuit voltage (OCV) . Limited ohmic losses were also observed for the test carried out with a CGO electrolyte supported cell (Series resistance, Rs=0.214 ohm cm^2 @ 0.7 V for a dense electrolyte of a thickness of about 250 μm). However, in this case, the maximum achievable performance was limited by the low OCV. The latter was due to the mixed conductivity phenomenon of CGO which corresponds to an internal current drag [83]. A different behavior was observed for the LSGM supporting cell. In this case, the achieved OCV was even higher than the thermodynamic value for water splitting at 800 °C. This aspect has been attributed to an additional oxygen pump effect which adds about 100 mV to the theoretical Nernst potential for the main reaction [84]. Despite this advantageous OCV value, the achieved performance was affected by a slight higher ohmic resistance (Rs=0.32 ohm cm^2 @ 0.7 V achieved with a dense electrolyte of a thickness of about 300 μm). Such lower performances for the electrolyte-supported SOFCs can be mitigated by reducing the electrolyte thickness, since the oxygen ion conductivities of CGO and LSGM are similar and better than the YSZ used in the Elcogen modified cell [8,54,85]. However, this should not occur at the expenses of the mechanical robustness. It is pointed out that the thickness of the overall anode-supported Elecogen cell is much larger than the electrolyte supported cells. But the excellent electronic conductivity of the anode support avoids the occurrence of relevant ohmic losses.

Another positive aspect associated to the use of LSGM consists on the possibility of achieving a proper mechanical and chemical compatibility with the exsolved perovskite being characterised by a similar structure and allowing the formation of a complete peroviste-structure based cell [54]. The polarization curve obtained with a protonic BYCO electrolyte indicates a proper OCV denoting an optimal sealing of cell and the presence of an additional oxygen conductivity for this electrolyte. In this case, no electronic drag associated to the redox behavior of cerium species occur since it Ce^{4+} is stabilized in the orthorhombic phase of the perovskite [86,87]. However, the performance achieved for the BYCO-based cell was strongly affected by large ohmic losses (1.44 ohm cm^2 @ 0.7 V for a dense electrolyte with a thickness of about 300 μm). This was in part due to the carbonation reaction of Ba generally occurring during the severe thermal treatment needed for its densification (above 1300 °C) which promotes the formation of an insulating phase [88,89]. The figure 3b shows the first derivate of the I-V curves of fig.3a highlighting the change of area surface resistance vs. the current density. It is noteworthy that the typical activation control at low current density is almost absent for all

experiments except the case of the experiment carried out with LSGM electrolyte. In this case, a fast decrease of resistance occurred during the first 300 mA cm^{-2} and this is due to the extra potential (about 100 mV) caused by the oxygen pump effect discussed above. By observing the ASR curve of experiment carried out the BYCO electrolyte, a stable and high resistance constraint was observed, confirming the evidences reported above. According to these experiments, the exsolved perovskite may be properly used as an anode for SOFCs fed with H_2 provided it is combined with a proper electrolyte material. In the case of the Elcogen-modified cell a peak power density of 1.4 W cm^{-2} is achieved whereas at 0.8 V the current density largely exceeds 1 W cm^{-2}.

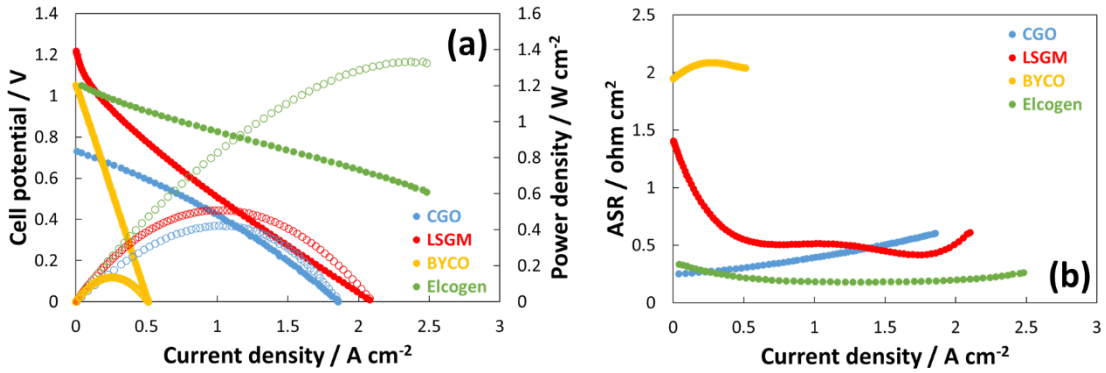

Figure 3. Polarisation and ASR curves at 800 °C for the modified perovskite-based cells fed with H_2 using three supporting electrolyte based SOFCs (e.g. CGO, LSGM, and BYCO) and a commercial Elcogen cell coated at the anode with an exsolved perovskite pre-layer. (a) cell potential and power densities vs and current density; (b) area specific resistance vs current density.

However, the modified perovskite catalysts have been mainly developed for the electro-oxidation of organic compounds with the aim to develop a fuel-flexible SOFC cell. Experiments reported in the literature have concerned the use of dry fuels (e.g. methane, syngas, methanol, ethanol, propane, and glycerol). Polarisation curves for the modified perovskite-based cells directly fed with various organic fuels are shown in figs 4a and 4b. One of the first reports addressing fuel flexibility was published in 2012 [52]. Electrochemical tests dealing with direct oxidation of various dry organic fuels were carried out for about 130 h without any relevant evidence of carbon formation. Fig. 4a shows the cell performance behavior for direct oxidation of several organic fuels using a thick (250 μm) CGO-electrolyte supported cell containing a modified-perovskite anode. The best performance is achieved for syngas, propane and methanol. Whereas low performance is observed for methane. However, despite the large thickness of the supporting electrolyte, the influence of the internal redox properties of the ceria based electrolyte ($Ce^{4+} \rightarrow Ce^{3+}$), in the presence of a reducing environment at the anode, dominates the polarization behavior.

As consequence, the observed OCV values are below 1 V for all experiments shown in Fig. 4a denoting an internal electronic drag due to the CGO redox properties [83], as discussed above. Moreover, the performances are also negatively affected by the thickness of CGO electrolyte.

The low performance achieved in the presence of dry methane is related to a poor reactivity of this molecule over the modified perovskite surface as corroborated by the low OCV. In this case, the polarization curve is strongly affected by both activation and ohmic constrains. Differently, from other organic fuels, direct methane oxidation appears quite difficult at the perovskite surface as confirmed by ex-situ catalytic tests carried under authothermal reforming (ATR) mode for methane [52].

Despite these limitations, the overall stability shown by this cell configuration during endurance tests with dry organic fuels was promising and prompted for further investigation with more appropriate cell designs. Fig. 4b summarizes some polarization curves achieved with different dry organic fuels and cell designs all based on modified perovskite anodes. One can observe that the cell designs can dramatically affect the performance. Ceria-based electrolytes show poor performance as consequence of significant electronic drag and low OCV, anode supported cell with thin YSZ electrolyte show the

best performance even if the OCV is slightly lower than that of the equivalent cells fed with hydrogen, supporting LSGM electrolyte based cells shows excellent OCV but strong ohmic losses. Thus, the most appropriate approach is to coat Ni-YSZ anode-supported cells with a modified or exsolved perovskite pre-layer (protecting layer or conducive catalytic layer). This can enhance fuel flexibility without relevant modifications of the SOFC technology.

For most of cell configurations, maximum power densities are achieved at a potential around 0.5 V. This voltage is generally considered as the lower potential limit for SOFC operation. At lower voltages, the overall efficiency is dramatically affected by the reduced voltage efficiency. This indicates that further efforts should be addressed to improve the voltage efficiency of dry organic fuels-fed SOFC cells by further amelioration of the modified perovskite properties. Moreover, it is needed to acquire more insights into the poor reaction kinetics of methane oxidation at the perovskite catalyst surface to improve the anode characteristics.

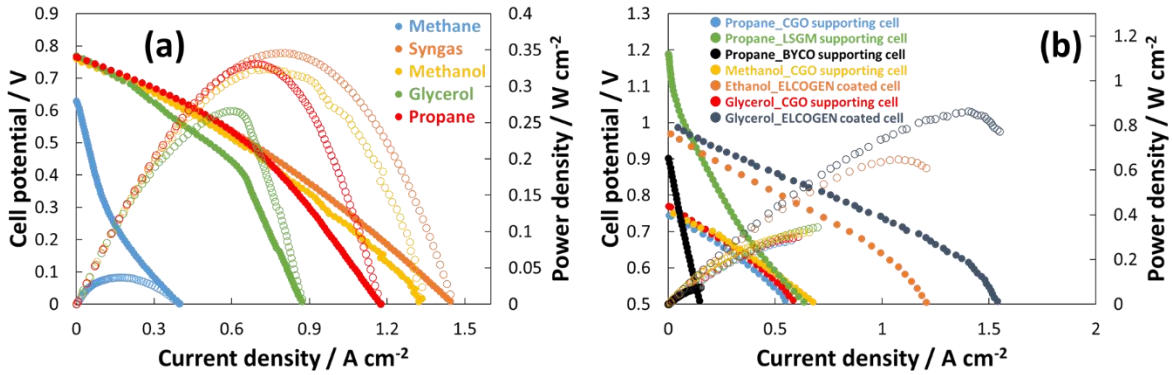

Figure 4. Polarisation curves for the modified perovskite-based cells operating in multifuel mode in the presence of a thick supported CGO electrolyte (a) [52] and with different organic fuels and cell designs (b) [49-51,54-56]

Several experiments carried out with organic fuels are summarized in table 2. In one cases, the exsolved perovskite has been studied for a 780 hrs in presence of a large excess of dry propane observing a decay of 1.1 10^{-4} A h^{-1}. In principle a large excess of fuel suppress the partial pressure of water and CO_2 formed during the electrochemical reaction occurring at the anode. As consequence, wet and dry reforming reaction are limited and the reactions causing the cracking of the organic fuel becomes largely probable. The open circuit voltage condition appears as the most stressful situation for the anode when this is fed with organic fuels. Therefore, demonstration of SOFC stability for a time exceeding 100 hrs under this condition is considered as very promising result.

Prolonged operation has not damaged the SOFC cell as well as the anode and there was no significant occurrence of carbon deposits on the surface [49]. Significant advances have regarded the use of this electrocatalyst as a coating layer of a commercial type cell fed directly with dry organic fuels as the ethanol and glycerol. The effective oxidation these fuels have confirmed the perspective that this electrocatalyst may have for the simplification of this technology, in particular of the balance of plant by reducing the fuel processing steps. Since the approach consisting in the use of a proper coating layer of modified perovskite on the anode, does not imply the modification of the SOFC production chain while making these devices fuel-flexible a proper diffusion of this approach is envisaged in the next years. Regarding the role of CGO mixed to the perovskite electrocatalyst, a previous paper [49] has elucidated the promoting effect of this mixed ionic electronically conducting material for propane oxidation.

In general, various results have demonstrated a strong increase of electro-catalytic activity in the presence of the exsolved perovskite. However, the activity is essentially related to the molecule structure and reactivity with the best results obtained with ethanol and propane (table 2). In particular, in the presence of methane in a test carried out with a CGO supported cell, a very low performance has been obtained [52]. The possible reasons for this behavior have been discussed at the light of electrochemical and chromatographic analysis results.

Table 2. Resume of the most important results of the electrochemical tests carried out at 800 °C with different organic fuels

	Type of cell / electrolyte	Maximum power density / mW cm^{-2}	Series resistance / Ω cm^{-2}	Total resistance / Ω cm^{-2}	Maximum durability demonstrated / h	Average decay during the life time test / A h^{-1}
Methane[52]	CGO (250 μm)	37 @ 0.22 V	0.51 @ 0.5 V	2.78 @ 0.5 V	15	0
Syngas[51]	CGO (250 μm)	346 @ 0.44 V	0.24 @ 0.765 V	0.29 @ 0.765 V	17[52]	0
Methanol[51]	CGO (250 μm)	358 @ 0.47 V	0.26 @ 0.75 V	0.33 @ 0.75 V	18[52]	$4\ 10^{-3}$
Ethanol[55]	Elcogen	648 @ 0.60 V	0.18 @ 0.7 V	0.46 @ 0.7 V	400	$1.5\ 10^{-4}$
Propane[49]	CGO (250 μm)	288 @ 0.51 V	0.25 @ 0.5 V	0.33 @ 0.5 V	780	$1.1\ 10^{-4}$
Propane[54]	LSGM (300 μm)	328 @ 0.43 V	0.32 @ 0.7 V	0.92 @ 0.7 V	15	$5\ 10^{-4}$
Glycerol[50]	CGO (250 μm)	320 @ 0.46 V	0.30 @ 0.5 V	0.66 @ 0.5 V	19[52]	0
Glycerol[56]	Elcogen	864 @ 0.62 V	0.12 @ 0.7 V	0.25 @ 0.7 V	157	$1\ 10^{-3}$

4. Reaction Mechanism

One important aspect of the previous studies carried out on modified perovskite electrocatalysts have regarded the reaction mechanisms involving the direct oxidation dry organic fuels [55,56]. Figure 5 depicts the mechanisms suggested for the electrochemical conversion of ethanol. The oxidation of dry ethanol appears to proceed through multiple and consequent reactions. These involve dehydrogenation and decomposition steps with consequent electrochemical oxidation of H_2 and CO to form water and CO_2 respectively. The latter processes occur at the triple phase boundaries. This mechanism has been named as "shuttle mechanism" to indicate iterative adsorption and desorption steps involving the reagent and the reaction intermediates. The side reforming reactions involving water and CO_2 also play a role even if in a lower extent in the presence of an excess of fuel. Such shuttle mechanism has been suggested based on a combination of chromatographic and HPLC (high performance liquid chromatography) studies carried out on the gaseous and liquid products for a cell operating with dry ethanol. These analyses have revealed the presence of acetaldehyde and acetic acid in addition to CH_4, CO_2, H_2O, and CO. These evidences has proved that one of the possible rate determining steps for this oxide catalyst regards the dehydrogenation. Therefore, it is largely probable that the cell fed with methane has shown lower performance being its dehydrogenation more difficult than other molecules. Also the oxidative coupling sometimes reported as a possible reaction catalyzed by perovskites[90] including the LSFC [47], may be reasonable neglected since no carbon based molecules with higher molecular weight than methane have been observed in the chromatographic analyses.

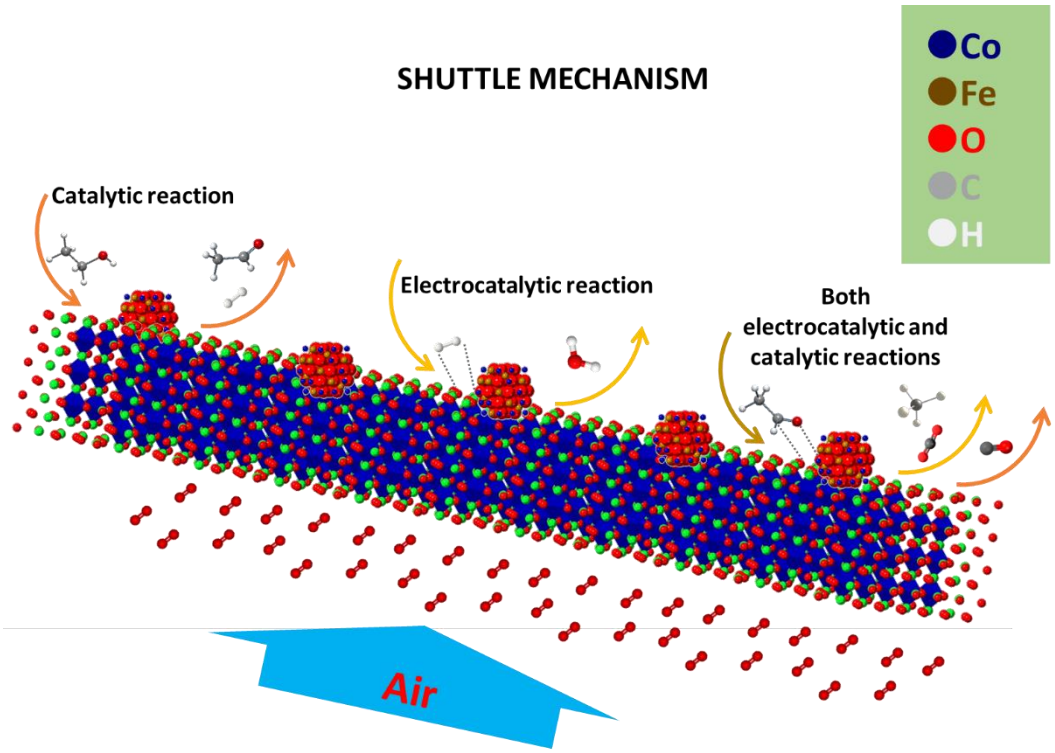

Figure 5. Exemplification of the shuttle mechanism suggested for dry ethanol fed at a modified perovskite–based SOFC cell. The support represents the exsolved perovskite whereas the fine embedded particles are ascribed to the α-Fe100-y-zCoyNizOx oxide. Air is fed to the cathode and oxygen ions migrate to the anode through the electrolyte.

5. Conclusions

The analysis presented in this mini-review deals with a number of studies carried out over more than a decade on a novel modified perovskite used as anode electrocatalyst for application in fuel-flexible SOFCs. The exsolved perovskite shows the presence of fine embedded particles made of transition elements such as Fe, Ni, Co over a depleted perovskite substrate. This structure is characterized by outstanding catalytic activity and proper electronic conductivity under reducing conditions. Moreover, a limited coarsening effect is generally observed for the nanoparticles even upon prolonged operation. Catalytic and the electrochemical studies have proved an effective capability of this material to convert organic fuels and good chemical stability under reducing conditions. These evidences make this electrocatalyst as a promising anode for electrolyte-supported cells or as coating layer for anode-supported cells. A specific "shuttle mechanism" is envisaged for the catalyst operation in a SOFC. This includes iterative adsorption and desorption steps involving the organic fuel and the reaction intermediates, the reaction at the interface of the formed hydrogen and carbon monoxide with the final formation of water and CO_2. This approach appears very promising for multi-fuels fed SOFCs and it is expected to be deserved of large interest in the coming years.

Author Contributions: conceptualization, A.S.A. and M.L.F.; methodology, A.S.A. and S.C.Z; software, M.L.F..; analysis, S.C.Z. and M.L.F.; investigation, S.C.Z.; writing—original draft preparation, M.L.F and A.S.A..; writing—review and editing, M.L.F. and A.S.A.; project administration, A.S.A.; funding acquisition, A.S.A.. All authors have read and agreed to the published version of the manuscript.

Funding: This research was funded by the Italian Ministry of Education, University and Research in the framework of PRIN2017 program and for the project entitled "Direct utilization of bio-fuels in solid oxide fuel

cells for sustainable and decentralised production of electric power and heat (DIRECTBIOPOWER)" Grant Agreement number: 2017FCFYHK.

Conflicts of Interest: The authors declare no conflict of interest.

References

1. Dong, Y.; Steinberg, M. Hynol--An economical process for methanol production from biomass and natural gas with reduced CO2 emission. *International Journal of Hydrogen Energy 22*, 971-977, doi:10.1016/s0360-3199(96)00198-x.
2. Gibbs, C.E.; Steel, M.C.F. European opportunities for fuel cell commercialisation. *Journal of Power Sources* **1992**, *37*, 35-43, doi:10.1016/0378-7753(92)80061-F.
3. Lee, A.L.; Zabransky, R.F.; Huber, W.J. Internal reforming development for Solid Oxide Fuel Cells. *Industrial and Engineering Chemistry Research* **1990**, *29*, 766-773, doi:10.1021/ie00101a009.
4. Bove, R.; Sammes, N.M. Thermodynmic analysis of SOFC systems using different fuel processors. In Proceedings of Fuel Cell Science, Engineering and Technology - 2004; pp. 461-466.
5. Steele, B.C.H. Materials for IT-SOFC stacks - 35 years R&D: The inevitability of gradualness? *Solid State Ionics* **2000**, *134*, 3-20, doi:10.1016/S0167-2738(00)00709-8.
6. La Rosa, D.; Lo Faro, M.; Monforte, G.; Antonucci, V.; Arico, A.S. Comparison of the electrochemical properties of intermediate temperature solid oxide fuel cells based on protonic and anionic electrolytes. *Journal of Applied Electrochemistry* **2009**, *39*, 477-483, doi:10.1007/s10800-008-9668-2.
7. Sauvert, A.L.; Fouletier, J. Research trends: Electrochemical properties of new type of IT-SOFC anode material. *Fuel Cells Bulletin* **2002**, *2002*, 12.
8. Lo Faro, M.; La Rosa, D.; Antonucci, V.; Arico, A.S. Intermediate temperature solid oxide fuel cell electrolytes. *Journal of the Indian Institute of Science* **2009**, *89*, 363-380.
9. Kikuchi, R.; Koashi, N.; Matsui, T.; Eguchi, K.; Norby, T. Novel anode materials for multi-fuel applicable solid oxide fuel cells. *Journal of Alloys and Compounds* **2006**, *408-412*, 622-627, doi:10.1016/j.jallcom.2004.12.179.
10. Lo Faro, M.; La Rosa, D.; Monforte, G.; Antonucci, V.; Arico, A.S.; Antonucci, P. Propane conversion over a Ru/CGO catalyst and its application in intermediate temperature solid oxide fuel cells. *Journal of applied electrochemistry* **2007**, *37*, 203-208.
11. La Rosa, D.; Sin, A.; Lo Faro, M.; Monforte, G.; Antonucci, V.; Arico, A.S. Mitigation of carbon deposits formation in intermediate temperature solid oxide fuel cells fed with dry methane by anode doping with barium. *Journal of Power Sources* **2009**, *193*, 160-164.
12. Lo Faro, M.; La Rosa, D.; Frontera, P.; Antonucci, P.; Antonucci, V.; Arico, A.S. Propane-fed Solid Oxide Fuel Cell based on a composite Ni-La-CGO anode catalyst. *Catalysis Letters* **2010**, *136*, 57-64, doi:10.1007/s10562-010-0295-2.
13. De Marco, V.; Iannaci, A.; Lo Faro, M.; Sglavo, V.M. Influence of Copper-based anode composition on intermediate temperature Solid Oxide Fuel Cells performance. *Fuel Cells* **2017**, *17*, 708-715, doi:10.1002/fuce.201700020.
14. Gandiglio, M.; Lanzini, A.; Santarelli, M.; Acri, M.; Hakala, T.; Rautanen, M. Results from an industrial size biogas-fed SOFC plant (the DEMOSOFC project). *International Journal of Hydrogen Energy* **2020**, *45*, 5449-5464, doi:10.1016/j.ijhydene.2019.08.022.

15. Yokokawa, H.; Suzuki, M.; Yoda, M.; Suto, T.; Tomida, K.; Hiwatashi, K.; Shimazu, M.; Kawakami, A.; Sumi, H.; Ohmori, M., et al. Achievements of NEDO durability projects on SOFC stacks in the light of physicochemical mechanisms. *Fuel Cells* **2019**, *19*, 311-339, doi:10.1002/fuce.201800187.
16. Santhanam, S.; Ullmer, D.; Wuillemin, Z.; Varkaraki, E.; Beetschen, C.; Antonetti, Y.; Ansar, A. Experimental analysis of a 25 kWe solid oxide fuel cell module for co-generation of hydrogen and power. In Proceedings of ECS Transactions; pp. 159-166.
17. McPhail, S.J.; Pumiglia, D.; Laurencin, J.; Hagen, A.; Leon, A.; Van Herle, J.; Vladikova, D.; Montinaro, D.; Piccardo, P.; Polverino, P., et al. Developing accelerated stress test protocols for solid oxide fuel cells and electrolysers: the European project AD ASTRA. In Proceedings of ECS Transactions; pp. 563-570.
18. Wang, Q.; Wei, H.H.; Xu, Q. A solid oxide fuel cell (SOFC)-based biogas-from-waste generation system for residential buildings in China: A feasibility study. *Sustainability (Switzerland)* **2018**, *10*, doi:10.3390/su10072395.
19. Stoeckl, B.; Subotić, V.; Preininger, M.; Schroettner, H.; Hochenauer, C. SOFC operation with carbon oxides: experimental analysis of performance and degradation. *Electrochimica Acta* **2018**, *275*, 256-264, doi:10.1016/j.electacta.2018.04.036.
20. Maraver, D.; Tondi, G.; Goodchild, R. Overview and current status of eu funded actions on bio-fuelled heating and combined heating & power within the energy challenge of Horizon 2020. In Proceedings of European Biomass Conference and Exhibition Proceedings; pp. 1289-1298.
21. Montinaro, D.; Sglavo, V.M.; Bertoldi, M.; Zandonella, T.; Aricò, A.; Lo Faro, M.; Antonucci, V. Tape casting fabrication and co-sintering of solid oxide "half cells" with a cathode–electrolyte porous interface. *Solid State Ionics* **2006**, *177*, 2093-2097.
22. Murata, K.; Shimotsu, M. Fabrication and evaluation of electrode-supported planar SOFC. *Denki Kagaku* **1997**, *65*, 38-43.
23. Wincewicz, K.C.; Cooper, J.S. Taxonomies of SOFC material and manufacturing alternatives. *Journal of Power Sources* **2005**, *140*, 280-296, doi:10.1016/j.jpowsour.2004.08.032.
24. Singh, D.; Hernández-Pacheco, E.; Hutton, P.N.; Patel, N.; Mann, M.D. Carbon deposition in an SOFC fueled by tar-laden biomass gas: a thermodynamic analysis. *Journal of Power Sources* **2005**, *142*, 194-199, doi:10.1016/j.jpowsour.2004.10.024.
25. Grgicak, C.M.; Green, R.G.; Giorgi, J.B. SOFC anodes for direct oxidation of hydrogen and methane fuels containing H_2S. *Journal of Power Sources* **2008**, *179*, 317-328, doi:10.1016/j.jpowsour.2007.12.082.
26. Schluckner, C.; Subotić, V.; Lawlor, V.; Hochenauer, C. Carbon deposition simulation in porous SOFC anodes: a detailed numerical analysis of major carbon precursors. *Journal of Fuel Cell Science and Technology* **2015**, *12*, doi:10.1115/1.4031862.
27. Fernandes, M.D.; Bistritzki, V.; Domingues, R.Z.; Matencio, T.; Rapini, M.; Sinisterra, R.D. Solid oxide fuel cell technology paths: national innovation system contributions from Japan and the United States. *Renewable and Sustainable Energy Reviews* **2020**, *127*, doi:10.1016/j.rser.2020.109879.
28. Lo Faro, M.; Trocino, S.; Zignani, S.C.; Aricò, A.S.; Maggio, G.; Italiano, C.; Fabiano, C.; Pino, L.; Vita, A. Study of a Solid Oxide Fuel Cell fed with n-dodecane reformate. Part I: Endurance test. *International Journal of Hydrogen Energy* **2016**, *41*, 5741-5747, doi:http://dx.doi.org/10.1016/j.ijhydene.2016.02.119.
29. Lo Faro, M.; Trocino, S.; Zignani, S.C.; Italiano, C.; Vita, A.; Aricò, A.S. Study of a solid oxide fuel cell fed with n-dodecane reformate. Part II: Effect of the reformate composition. *International Journal of Hydrogen Energy* **2017**, *42*, 1751-1757, doi:10.1016/j.ijhydene.2016.06.048.
30. Zhan, Z.; Lin, Y.; Bamett, S. Anode catalyst layers for direct hydrocarbon and internal reforming SOFCs. In Proceedings of Proceedings - Electrochemical Society; pp. 1321-1330.

31. Lo Faro, M.; Reis, R.M.; Saglietti, G.G.A.; Sato, A.G.; Ticianelli, E.A.; Zignani, S.C.; Aricò, A.S. Nickel-Copper/Gadolinium-doped Ceria (CGO) composite electrocatalyst as a protective layer for a Solid-Oxide Fuel Cell anode fed with ethanol. *ChemElectroChem* **2014**, *1*, 1395-1402, doi:10.1002/celc.201402017.
32. Lo Faro, M.; Reis, R.M.; Saglietti, G.G.A.; Zignani, S.C.; Trocino, S.; Frontera, P.; Antonucci, P.L.; Ticianelli, E.A.; Aricò, A.S. Investigation of Ni-based alloy/CGO electro-catalysts as protective layer for a solid oxide fuel cell anode fed with ethanol. *Journal of Applied Electrochemistry* **2015**, *45*, 647-656, doi:10.1007/s10800-015-0849-5.
33. Lo Faro, M.; Trocino, S.; Zignani, S.C.; Italiano, C.; Reis, R.M.; Ticianelli, E.A.; Aricò, A.S. Nickel–Iron/Gadolinium-doped Ceria (CGO) composite electrocatalyst as a protective layer for a Solid-Oxide Fuel Cell anode fed with biofuels. *ChemCatChem* **2016**, *8*, 648-655, doi:10.1002/cctc.201501090.
34. Li, J.; Croiset, E.; Ricardez-Sandoval, L. Theoretical investigation of the methane cracking reaction pathways on Ni (1 1 1) surface. *Chemical Physics Letters* **2015**, *639*, 205-210, doi:10.1016/j.cplett.2015.09.030.
35. Lo Faro, M.; Frontera, P.; Antonucci, P.; Aricò, A.S. Ni-Cu based catalysts prepared by two different methods and their catalytic activity toward the ATR of methane. *Chemical Engineering Research and Design* **2015**, *93*, 269-277, doi:10.1016/j.cherd.2014.05.014.
36. Laosiripojana, N.; Assabumrungrat, S. The effect of specific surface area on the activity of nano-scale ceria catalysts for methanol decomposition with and without steam at SOFC operating temperatures. *Chemical Engineering Science* **2006**, *61*, 2540-2549, doi:10.1016/j.ces.2005.11.024.
37. Ioselevich, A.; Kornyshev, A.A.; Lehnert, W. Statistical geometry of reaction space in porous cermet anodes based on ion-conducting electrolytes patterns of degradation. *Solid State Ionics* **1999**, *124*, 221-237, doi:10.1016/S0167-2738(99)00218-0.
38. Crosbie, G.M.; Murray, E.P.; Bauer, D.R.; Kim, H.; Park, S.; Vohs, J.M.; Gorte, R.J. Solid oxide fuel cells for direct oxidation of liquid hydrocarbon fuels in automotive auxiliary power units: Sulfur tolerance and operation on gasoline. *SAE Technical Papers* **2002**, 10.4271/2002-01-0410, doi:10.4271/2002-01-0410.
39. Mogensen, M. Direct conversion of hydrocarbons in Solid Oxide Fuel Cells: a review. In Proceedings of ACS Division of Fuel Chemistry, Preprints; p. 498.
40. Sun, Y.F.; Zhou, X.W.; Zeng, Y.; Amirkhiz, B.S.; Wang, M.N.; Zhang, L.Z.; Hua, B.; Li, J.; Li, J.H.; Luo, J.L. An ingenious Ni/Ce co-doped titanate based perovskite as a coking-tolerant anode material for direct hydrocarbon solid oxide fuel cells. *Journal of Materials Chemistry A* **2015**, *3*, 22830-22838, doi:10.1039/c5ta06200d.
41. Yu Yao, Y.F. The oxidation of hydrocarbons and CO over metal oxides. IV. Perovskite-type oxides. *Journal of Catalysis* **1975**, *36*, 266-275, doi:10.1016/0021-9517(75)90036-6.
42. Shimizu, T. Partial oxidation of hydrocarbons and oxygenated compounds on perovskite oxides. *Catalysis Reviews* **1992**, *34*, 355-371, doi:10.1080/01614949208016317.
43. Niu, B.; Jin, F.; Yang, X.; Feng, T.; He, T. Resisting coking and sulfur poisoning of double perovskite $Sr_2TiFe_{0.5}Mo_{0.5}O_{6-\Delta}$ anode material for solid oxide fuel cells. *International Journal of Hydrogen Energy* **2018**, *43*, 3280-3290, doi:10.1016/j.ijhydene.2017.12.134.
44. Swartz, S.L. Sulfur tolerant fuel processing catalysts. In Proceedings of ACS National Meeting Book of Abstracts.
45. Wang, S.; Jiang, Y.; Zhang, Y.; Li, W.; Yan, J.; Lu, Z. Electrochemical performance of mixed ionic-electronic conducting oxides as anodes for solid oxide fuel cell. *Solid State Ionics* **1999**, *120*, 75-84, doi:10.1016/S0167-2738(98)00558-X.
46. Sammes, N.M.; Ratnaraj, R. High-temperature mechanical properties of $La_{0.7}Sr_{0.3}Cr_{1-y}Co_yO_3$ in reducing environments. *J Mater Sci* **1997**, *32*, 687-692, doi:10.1023/A:1018591803417.

47. Xu, S.J.; Thomson, W.J. Stability of $La_{0.6}Sr_{0.4}Co_{0.2}Fe_{0.8}O_{3-\delta}$ perovskite membranes in reducing and nonreducing environments. *Industrial and Engineering Chemistry Research* **1998**, *37*, 1290-1299.
48. Zhang, Y.; Sun, Y.F.; Luo, J.L. Ce/Ni decorated titanate based perovskite for solid oxide fuel cells. In Proceedings of ECS Transactions; pp. 91-97.
49. Lo Faro, M.; La Rosa, D.; Nicotera, I.; Antonucci, V.; Arico, A.S. Electrochemical investigation of a propane-fed solid oxide fuel cell based on a composite Ni-perovskite anode catalyst. *Applied Catalysis B-Environmental* **2009**, *89*, 49-57, doi:10.1016/j.apcatb.2008.11.019.
50. Lo Faro, M.; Minutoli, M.; Monforte, G.; Antonucci, V.; Arico, A.S. Glycerol oxidation in solid oxide fuel cells based on a Ni-perovskite electrocatalyst. *Biomass & Bioenergy* **2011**, *35*, 1075-1084, doi:10.1016/j.biombioe.2010.11.018.
51. Lo Faro, M.; Stassi, A.; Antonucci, V.; Modafferi, V.; Frontera, P.; Antonucci, P.; Arico, A.S. Direct utilization of methanol in solid oxide fuel cells: an electrochemical and catalytic study. *International Journal of Hydrogen Energy* **2011**, *36*, 9977-9986, doi:10.1016/j.ijhydene.2011.05.053.
52. Lo Faro, M.; Antonucci, V.; Antonucci, P.L.; Aricò, A.S. Fuel flexibility: a key challenge for SOFC technology. *Fuel* **2012**, *102*, 554-559.
53. Lo Faro, M.; Modafferi, V.; Frontera, P.; Antonucci, P.; Aricò, A.S. Catalytic behavior of Ni-modified perovskite and doped ceria composite catalyst for the conversion of odorized propane to syngas. *Fuel Processing Technology* **2013**, *113*, 28-33.
54. Lo Faro, M.; Arico, A.S. Electrochemical behaviour of an all-perovskite-based intermediate temperature solid oxide fuel cell. *International Journal of Hydrogen Energy* **2013**, *38*, 14773-14778, doi:10.1016/j.ijhydene.2013.08.122.
55. Lo Faro, M.; Reis, R.M.; Saglietti, G.G.A.; Oliveira, V.L.; Zignani, S.C.; Trocino, S.; Maisano, S.; Ticianelli, E.A.; Hodnik, N.; Ruiz-Zepeda, F., et al. Solid oxide fuel cells fed with dry ethanol: The effect of a perovskite protective anodic layer containing dispersed Ni-alloy @ FeOx core-shell nanoparticles. *Applied Catalysis B: Environmental* **2018**, *220*, 98-110, doi:https://doi.org/10.1016/j.apcatb.2017.08.010.
56. Lo Faro, M.; Oliveira, V.L.; Reis, R.M.; Saglietti, G.G.A.; Zignani, S.C.; Trocino, S.; Ticianelli, E.A.; Aricò, A.S. Solid Oxide Fuel Cell fed directly with dry glycerol. *Energy Technology* **2019**, *7*, 45-47, doi:doi:10.1002/ente.201700744.
57. Jardiel, T.; Caldes, M.T.; Moser, F.; Hamon, J.; Gauthier, G.; Joubert, O. New SOFC electrode materials: the Ni-substituted LSCM-based compounds $(La_{0.75}Sr_{0.25})(Cr_{0.5}Mn_{0.5-x}Ni_x)O_{3-\delta}$ and $(La_{0.75}Sr_{0.25})(Cr_{0.5-x}Ni_xMn_{0.5})O_{3-\delta}$. *Solid State Ionics* **2010**, *181*, 894-901, doi:10.1016/j.ssi.2010.05.012.
58. Van Den Bossche, M.; McIntosh, S. Pulse reactor studies to assess the potential of $La_{0.75}Sr_{0.25}Cr_{0.5}Mn_{0.4}X_{0.1}O_{3-\delta}$ (X = Co, Fe, Mn, Ni, V) as direct hydrocarbon solid oxide fuel cell anodes. *Chemistry of Materials* **2010**, *22*, 5856-5865, doi:10.1021/cm101567v.
59. Lay, E.; Gauthier, G.; Dessemond, L. Preliminary studies of the new Ce-doped La/Sr chromo-manganite series as potential SOFC anode or SOEC cathode materials. *Solid State Ionics* **2011**, *189*, 91-99, doi:10.1016/j.ssi.2011.02.004.
60. Vecino-Mantilla, S.; Gauthier-Maradei, P.; Huvé, M.; Serra, J.M.; Roussel, P.; Gauthier, G.H. Nickel exsolution-driven phase transformation from an n=2 to an n=1 Ruddlesden-Popper manganite for methane Steam Reforming reaction in SOFC conditions. *ChemCatChem* **2019**, *11*, 4631-4641, doi:10.1002/cctc.201901002.
61. Hou, N.; Yao, T.; Li, P.; Yao, X.; Gan, T.; Fan, L.; Wang, J.; Zhi, X.; Zhao, Y.; Li, Y. A-site ordered double perovskite with in situ exsolved core-shell nanoparticles as anode for solid oxide fuel cells. *ACS Applied Materials and Interfaces* **2019**, *11*, 6995-7005, doi:10.1021/acsami.8b19928.

62. Lo Faro, M.; La Rosa, D.; Nicotera, I.; Antonucci, V.; Aricò, A.S. Electrochemical behaviour of propane-fed solid oxide fuel cells based on low Ni content anode catalysts. *Electrochimica Acta* **2009**, *54*, 5280-5285.
63. Vecino-Mantilla, S.; Quintero, E.; Fonseca, C.; Gauthier, G.H.; Gauthier-Maradei, P. Catalytic steam reforming of natural gas over a new Ni exsolved Ruddlesden-Popper manganite in SOFC anode conditions. *ChemCatChem* **2020**, *12*, 1453-1466, doi:10.1002/cctc.201902306.
64. Kim, J.S.; Lee, J.Y.; Swinnea, J.S.; Steinfink, H.; Reiff, W.M.; Lightfoot, P.; Pei, S.; Jorgensen, J.D. Ruddlesden-Popper phases $A_{n+1}M_nO_{3n+1}$. Structures and properties. *NIST Special Publication* **1991**, 301-306.
65. Smith, R.D.L.; Prévot, M.S.; Fagan, R.D.; Zhang, Z.; Sedach, P.A.; Siu, M.K.J.; Trudel, S.; Berlinguette, C.P. Photochemical Route for Accessing Amorphous Metal Oxide Materials for Water Oxidation Catalysis. *Science* **2013**, *340*, 60-63, doi:10.1126/science.1233638.
66. Smith, R.D.L.; Prévot, M.S.; Fagan, R.D.; Trudel, S.; Berlinguette, C.P. Water oxidation catalysis: electrocatalytic response to metal stoichiometry in amorphous metal oxide films containing Iron, Cobalt, and Nickel. *Journal of the American Chemical Society* **2013**, *135*, 11580-11586, doi:10.1021/ja403102j.
67. Tang, C.-W.; Wang, C.-B.; Chien, S.-H. Characterization of cobalt oxides studied by FT-IR, Raman, TPR and TG-MS. *Thermochimica Acta* **2008**, *473*, 68-73, doi:https://doi.org/10.1016/j.tca.2008.04.015.
68. Tiernan, M.J.; Barnes, P.A.; Parkes, G.M.B. Reduction of Iron oxide catalysts: the Investigation of kinetic parameters using rate perturbation and linear heating thermoanalytical techniques. *The Journal of Physical Chemistry B* **2001**, *105*, 220-228, doi:10.1021/jp003189+.
69. Li, C.; Chen, Y.W. Temperature-programmed-reduction studies of nickel oxide/alumina catalysts: effects of the preparation method. *Thermochimica Acta* **1995**, *256*, 457-465, doi:10.1016/0040-6031(94)02177-P.
70. Marrero-Jerez, J.; Larrondo, S.; Rodríguez-Castellón, E.; Núñez, P. TPR, XRD and XPS characterisation of ceria-based materials synthesized by freeze-drying precursor method. *Ceramics International* **2014**, *40*, 6807-6814, doi:10.1016/j.ceramint.2013.11.143.
71. Steele, B.C.H. Oxygen transport and exchange in oxide ceramics. *Journal of Power Sources* **1994**, *49*, 1-14, doi:10.1016/0378-7753(93)01789-k.
72. Liu, D.J.; Krumpelt, M. Activity and structure of perovskites as diesel-reforming catalysts for solid oxide fuel cell. *International Journal of Applied Ceramic Technology* **2005**, *2*, 301-307, doi:10.1111/j.1744-7402.2005.02032.x.
73. Aguiar, P.; Lapeña-Rey, N.; Chadwick, D.; Kershenbaum, L. Improving catalyst structures and reactor configurations for autothermal reaction systems: application to solid oxide fuel cells. *Chemical Engineering Science* **2001**, *56*, 651-658, doi:10.1016/S0009-2509(00)00272-4.
74. Bastidas, D.M.; Irvine, J.T.S. LSCM based SOFC a suitable system for direct propane operation. In Proceedings of Proceedings of the 1st European Fuel Cell Technology and Applications Conference 2005 - Book of Abstracts; p. 150.
75. Cheekatamarla, P.K.; Finnerty, C.M.; Cai, J. Internal reforming of hydrocarbon fuels in tubular solid oxide fuel cells. *International Journal of Hydrogen Energy* **2008**, *33*, 1853-1858, doi:10.1016/j.ijhydene.2008.02.004.
76. Douvartzides, S.L.; Coutelieris, F.A.; Tsiakaras, P.E. Effect of reforming on the overall efficiency of a solid oxide fuel-cell based power plant system fed by methane. *International Journal of Exergy* **2004**, *1*, 179-188, doi:10.1504/IJEX.2004.005089.
77. Lo Faro, M.; Vita, A.; Pino, L.; Aricò, A.S. Performance evaluation of a solid oxide fuel cell coupled to an external biogas tri-reforming process. *Fuel Processing Technology* **2013**, *115*, 238-245.
78. Manenti, F.; Pelosato, R.; Vallevi, P.; Leon-Garzon, A.R.; Dotelli, G.; Vita, A.; Faro, M.L.; Maggio, G.; Pino, L.; Arico, A.S. Biogas-fed solid oxide fuel cell (SOFC) coupled to tri-reforming process: modelling and

simulation. *International Journal of Hydrogen Energy* **2015**, *40*, 14640-14650, doi:10.1016/j.ijhydene.2015.08.055.

79. Al-Qattan, A.M.; Chmielewski, D.J. Distributed feed design for SOFCs with internal reforming. *J. Electrochem. Soc.* **2004**, *151*, A1891-A1898, doi:10.1149/1.1802151.
80. Lim, L.T.; Chadwick, D.; Kershenbaum, L. Achieving autothermal operation in internally reformed solid oxide fuel cells: Simulation studies. *Industrial and Engineering Chemistry Research* **2005**, *44*, 9609-9618, doi:10.1021/ie050271o.
81. Georges, S.; Parrour, G.; Henault, M.; Fouletier, J. Gradual internal reforming of methane: A demonstration. *Solid State Ionics* **2006**, *177*, 2109-2112, doi:10.1016/j.ssi.2006.01.033.
82. De Lorenzo, G.; Corigliano, O.; Lo Faro, M.; Frontera, P.; Antonucci, P.; Zignani, S.C.; Trocino, S.; Mirandola, F.A.; Aricò, A.S.; Fragiacomo, P. Thermoelectric characterization of an intermediate temperature solid oxide fuel cell system directly fed by dry biogas. *Energy Conversion and Management* **2016**, *127*, 90-102, doi:10.1016/j.enconman.2016.08.079.
83. Leah, R.; Bone, A.; Selcuk, A.; Corcoran, D.; Lankin, M.; Dehaney-Steven, Z.; Selby, M.; Whalen, P. Development of highly robust, volume-manufacturable metal-supported SOFCs for operation below 600°C. In Proceedings of ECS Transactions; pp. 351-367.
84. Skinner, S.J.; Kilner, J.A. Oxygen ion conductors. *Materials Today* **2003**, *6*, 30-37, doi:https://doi.org/10.1016/S1369-7021(03)00332-8.
85. Lo Faro, M.; Arico, A.S. Ceramic membranes for intermediate temperature solid oxide fuel cells (SOFCs): state of the art and perspectives. In *Membranes for Clean and Renewable Power Applications*, Gugliuzza, A., Basile, A., Eds. Woodhead Publ Ltd: Cambridge, 2014; 10.1533/9780857098658.4.237pp. 237-265.
86. Coors, W.G. Protonic ceramic steam-permeable membranes. *Solid State Ionics* **2007**, *178*, 481-485, doi:10.1016/j.ssi.2006.11.004.
87. Oishi, M.; Akoshima, S.; Yashiro, K.; Sato, K.; Mizusaki, J.; Kawada, T. Defect structure analysis of B-site doped perovskite-type proton conducting oxide $BaCeO_3$. Part 2: The electrical conductivity and diffusion coefficient of $BaCe_{0.9}Y_{0.1}O_{3-\delta}$. *Solid State Ionics* **2008**, *179*, 2240-2247, doi:10.1016/j.ssi.2008.08.005.
88. Ivanova, M.; Ricote, S.; Baumann, S.; Meulenberg, W.A.; Tietz, F.; Serra, J.M.; Richter, H. Ceramic materials for energy and environmental applications: Functionalizing of properties by tailored compositions. In *Doping: Properties, Mechanisms and Applications*, 2013; pp. 221-276.
89. Giannici, F.; Longo, A.; Deganello, F.; Balerna, A.; Arico, A.S.; Martorana, A. Local environment of Barium, Cerium and Yttrium in $BaCe_{1-x}Y_xO_{3-\delta}$ ceramic protonic conductors. *Solid State Ionics* **2007**, *178*, 587-591, doi:10.1016/j.ssi.2007.01.015.
90. Shamsi, A.; Zahir, K. Oxidative-coupling of methane over Perovskite-type oxides and correlation of TMAX for oxygen desorption with C2 selectivity. *Preprints Symposia* **1989**, *34*, 544.